Biomedical Optics EXPRESS

Effects of speckle/pixel size ratio on temporal and spatial speckle-contrast analysis of dynamic scattering systems: Implications for measurements of blood-flow dynamics

J. C. Ramirez-San-Juan,[1,2,*] E. Mendez- Aguilar,[1] N. Salazar-Hermenegildo,[1] A. Fuentes-Garcia,[1] R. Ramos-Garcia,[1] and B. Choi[2,3,4]

[1] *Optics Department, INAOE, Puebla, Mexico*
[2] *Beckman Laser Institute and Medical Clinic, Department of Surgery, University of California, Irvine, 1002 Health Sciences Road East, Irvine, California 92612, USA*
[3] *Department of Biomedical Engineering, University of California, Irvine, 3120 Natural Sciences II, Irvine, California 92697, USA*
[4] *Edwards Life sciences Center for Advanced Cardiovascular Technology, University of California, Irvine, 2400 Engineering Hall, Irvine, California 92697, USA*
** jcram@inaoep.mx*

Abstract: Laser Speckle Contrast Imaging (LSCI) is an optical technique used to generate blood flow maps with high spatial and temporal resolution. It is well known that in LSCI, the speckle size must exceed the Nyquist criterion to maximize the speckle's pattern contrast. In this work, we study experimentally the effect of speckle-pixel size ratio not only in dynamic speckle contrast, but also on the calculation of the relative flow speed for temporal and spatial analysis. Our data suggest that the temporal LSCI algorithm is more accurate at assessing the relative changes in flow speed than the spatial algorithm.

OCIS codes: (120.6150) Speckle imaging; (120.7250) Velocimetry; (030.6140) Speckle.

References and links

1. J. W. Goodman, *Statistical Optics* (New York: Wiley, 1985).
2. F. Fercher and J. D. Briers, "Flow visualization by means of single-exposure speckle photography," Opt. Commun. **37**(5), 326–330 (1981).
3. O. Yang, D. Cuccia, and B. Choi, "Real-time blood flow visualization using the graphics processing unit," J. Biomed. Opt. **16**(1), 016009 (2011).
4. A. K. Dunn, "Laser speckle contrast imaging of cerebral blood flow," Ann. Biomed. Eng. **40**(2), 367–377 (2012).
5. W. J. Moy, S. J. Patel, B. S. Lertsakdadet, R. P. Arora, K. M. Nielsen, K. M. Kelly, and B. Choi, "Preclinical in vivo evaluation of NPe6-mediated photodynamic therapy on normal vasculature," Lasers Surg. Med. **44**(2), 158–162 (2012).
6. A. B. Parthasarathy, E. L. Weber, L. M. Richards, D. J. Fox, and A. K. Dunn, "Laser speckle contrast imaging of cerebral blood flow in humans during neurosurgery: a pilot clinical study," J. Biomed. Opt. **15**(6), 066030 (2010).
7. A. Humeau-Heurtier, B. Buard, G. Mahe, and P. Abraham, "Laser speckle contrast imaging of the skin: interest in processing the perfusion data," Med. Biol. Eng. Comput. **50**(2), 103–105 (2012).
8. S. J. Kirkpatrick, D. D. Duncan, and E. M. Wells-Gray, "Detrimental effects of speckle-pixel size matching in laser speckle contrast imaging," Opt. Lett. **33**(24), 2886–2888 (2008).
9. O. Thompson, M. Andrews, and E. Hirst, "Correction for spatial averaging in laser speckle contrast analysis," Biomed. Opt. Express **2**(4), 1021–1029 (2011).
10. A. Ennos, "Speckle interferometry," in *Laser Speckle and Related Phenomena,* J.C. Dainty (Springer-Verlag)
11. H. Y. Cheng, Q. M. Luo, S. Q. Zeng, S. B. Chen, J. Cen, and H. Gong, "Modified laser speckle imaging method with improved spatial resolution," J. Biomed. Opt. **8**(3), 559–564 (2003).
12. A. B. Parthasarathy, W. J. Tom, A. Gopal, X. Zhang, and A. K. Dunn, "Robust flow measurement with multi-exposure speckle imaging," Opt. Express **16**(3), 1975–1989 (2008).
13. D. A. Boas and A. K. Dunn, "Laser speckle contrast imaging in biomedical optics," J. Biomed. Opt. **15**(1), 011109 (2010).
14. P. A. Lemieux and D. J. Durian, "Investigating non-Gaussian scattering process by using nth-order intensity correlation function," J. Opt. Soc. Am. A **16**(7), 1651–1664 (1999).

#191144 - $15.00 USD Received 24 May 2013; revised 25 Jul 2013; accepted 26 Jul 2013; published 30 Aug 2013

15. Y. Atchia, H. Levy, S. Dufour, and O. Levi, "Rapid multiexposure in vivo brain imaging system using vertical cavity surface emitting lasers as a light source," Appl. Opt. **52**(7), C64–C71 (2013).
16. J. C. Ramirez-San-Juan, R. Ramos-García, I. Guizar-Iturbide, G. Martínez-Niconoff, and B. Choi, "Impact of velocity distribution assumption on simplified laser speckle imaging equation," Opt. Express **16**(5), 3197 (2008).
17. K. Basak, M. Manjunatha, and P. K. Dutta, "Review of laser speckle-based analysis in medical imaging," Med. Biol. Eng. Comput. **50**(6), 547–558 (2012).
18. D. D. Duncan, S. J. Kirkpatrick, and R. K. Wang, "Statistics of local speckle contrast," J. Opt. Soc. Am. A **25**(1), 9–15 (2008).
19. P. Li, S. Ni, L. Zhang, S. Zeng, and Q. Luo, "Imaging cerebral blood flow through the intact rat skull with temporal laser speckle imaging," Opt. Lett. **31**(12), 1824–1826 (2006).

1. Introduction

When coherent light is used to illuminate a rough or optically inhomogeneous object, the scattered light forms a random interference pattern called speckle [1]. In 1981, Fercher and Briers [2] demonstrated that analysis of the speckle contrast in a time-integrated speckle pattern enables visualization of blood flow in the retina. With subsequent advances in charge-coupled device (CCD) technology and an associated reduction in cost, LSCI method has been implemented in real time [3] and employed in numerous preclinical [4,5] and clinical [6] research studies as a simple method to quantify blood-flow dynamics [7].

The dynamic range of LSCI is closely related to the range of measurable speckle contrast values. This range itself is linked to several experimental parameters, including source coherence length, analysis algorithm approach (i.e., temporal vs. spatial analysis), and the spatial sampling (Fig. 1) of the speckle pattern [8, 9].

In this work, we focus on continuing the discussion related to the proper spatial sampling of speckle patterns, Fig. 1 shows several pixels which are sampling a speckle, the ratio speckle area/pixel area defines the parameter N employed in the following plots.

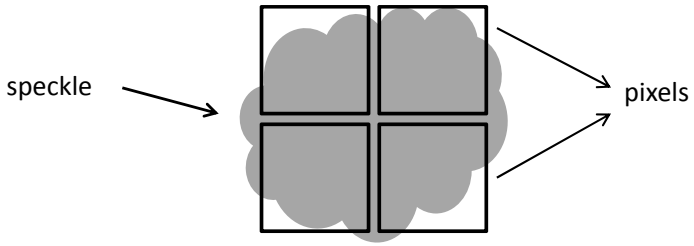

Fig. 1. Spatial sampling of a speckle pattern on a CCD camera.

The key governing equation involves the minimum-resolvable speckle size, d_{min}, which is related to the diffraction-limited equation used in optical imaging [9,10]:

$$d_{\min} = 1.22(1+M)(f/\#)\lambda \quad (1)$$

where M is the optical magnification, f/# the f-stop of the imaging optics, and λ the optical wavelength of the coherent source. Historically, experimental parameters were chosen to match approximately d_{min} with the pixel pitch of the imaging sensor. However, in order to satisfy the Nyquist sampling criterion and maximize the contrast of the imaged speckle pattern, Kirkpatrick *et al.* [8] used an *in-vitro* experimental setup to demonstrate that pixel size should be at least twice the pixel size. This finding was supported by computer simulation data from Thompson *et al.* [9].

The data from Kirkpatrick *et al.* [8] represent one extreme condition, in which the speckle pattern consists solely of static speckle. However, in biological samples, a mixture of static and dynamic contributions to the imaged speckle pattern is expected. As a consequence, blurring of the image and subsequent decrease of the maximum achievable speckle contrast due to spatial and temporal integration of the light is produced. In this work, we present *in-vitro* experimental data that support this concept and discuss the implications for LSI-based characterization of dynamic scattering systems.

#191144 - $15.00 USD Received 24 May 2013; revised 25 Jul 2013; accepted 26 Jul 2013; published 30 Aug 2013

2. Materials and methods

2.1 Flow phantom

The flow phantom (Fig. 2) consists of a micro-channel slide (thinXXS Microtechnology AG) with channels of 300-µm diameter. The slide was placed on a rigid resin substrate polymerized with a suspension of TiO_2 particles to simulate the scattering properties of human skin. A syringe-based infusion pump was used to induce flow of 1% Intralipid through the channels, at flow speeds from 4 to 20 mm/s in step of 2 mm/sec.

2.2 Laser speckle contrast imaging (LSCI)

An expanded and collimated 532-nm laser (Verdi, Coherent Inc.) illuminates an engineered diffuser, which in turn, homogenously illuminates the flow phantom. Raw speckle images were acquired with a Retiga CCD camera (7.4µm x 7.4µm pixel area) equipped with a macro lens with variable aperture. A linear polarizer was placed in front of the camera lens and its orientation is set to be perpendicular to that of the incident light's polarization to minimize specular reflection from the skin phantom. In order to modulate the speckle's size, and therefore the speckle/pixel size ratio, we changed the f/# setting of the lens (Eq. (1)), and the laser power was adjusted to achieve a consistent mean gray level measured from the CCD sensor. The exposure time was fixed at 10 ms because this value is common for in-vivo LSI applications.

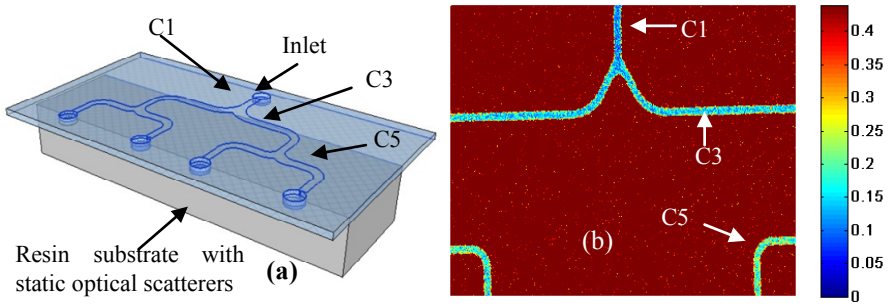

Fig. 2. (a) Skin phantom employed in this study. Intralipid was injected into the inlet. K (contrast) and SFI (Speckle Flow Index) measurements were determined at regions within channels C1, C3 and C5. (b) Representative speckle contrast image of the skin phantom during flow at 6 mm/sec. See text for details.

2.3 Experimental design and data analysis

For each flow-speed setting, we collected a sequence of 30 raw speckle images. The sequences were processed using either temporal [11] or spatial [2] algorithms to calculate resultant speckle-contrast images. The temporal algorithm, analysis was done on a pixel-by-pixel basis, using the previously-published temporal LSI algorithm [11]. While for the spatial algorithm, each of the 30 images were converted to corresponding speckle-contrast images, using a 5 × 5 sliding-window operator, and an average speckle contrast image was calculated. With the resultant speckle-contrast images, we focused our analysis on 30 × 100 regions of interest within channels C1, C3 and C5.

Parthasarathy *et al.* [12] and Boas *et al.* [13] derived an equation that relates speckle contrast (K) and the correlation time (τ_c) of the backscattered light from the sample:

$$K(T,\tau_c)=\left[\beta\rho^2\frac{e^{-2x}-1+2x}{2x^2}+4\beta\rho(1-\rho)\frac{e^{-x}-1+x}{x^2}+(1-\rho)^2\right]^{1/2}+C_{noise} \quad (2)$$

where $x = T/\tau_C$, T is the camera exposure time, $\rho = I_f/(I_f + I_s)$ is the fraction of total light that is scattered by moving optical scatterers, C_{noise} is a constant term that accounts for noise [12],

#191144 - $15.00 USD Received 24 May 2013; revised 25 Jul 2013; accepted 26 Jul 2013; published 30 Aug 2013

and β accounts for the effect of spatial integration of the speckle pattern due to the finite size of the pixel [14,15]. In the absence of static optical scatterers (ρ →1) and noise (C_{noise}→0), Eq. (2) simplifies to [12]:

$$K(T,\tau_c)=\left[\beta\frac{e^{-2x}-1+2x}{2x^2}\right]^{1/2} \tag{3}$$

In the long exposure regime (i.e., T >> τ_c) [16] and considering that the flow speed V∝ $1/\tau_c$≡SFI, where SFI is Speckle Flow Index [17], Eq. (3) can be approximated as:

$$K=aV^{-1/2} \tag{4}$$

where *a* is a proportionality constant. In [12] the authors reported τ_c values in the order of microseconds, in our experiments the exposure time is 10 ms, it means that the experiments developed in this work are in the long exposure regime and therefore we can use Eq. (4).

3. Results and discussion

Figure 3 shows the average speckle contrast of a region within channel C1 obtained with the temporal (Fig. 3(a)) and the spatial (Fig. 3(b)) contrast analysis as a function of the actual flow speed, for different values of N, which is the number of pixels per speckle (Fig. 1).

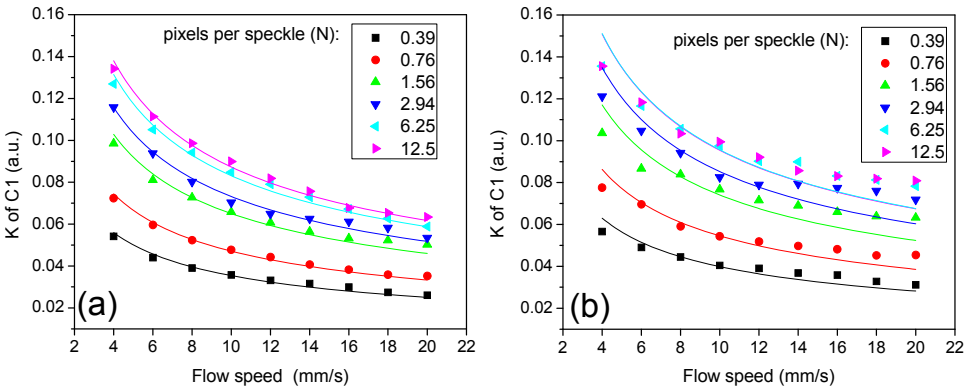

Fig. 3. Average speckle contrast of a region within channel C1, vs. flow speed, for different ratios of spatial sampling of the speckle pattern (i.e., "pixels-per-speckle" values) for (a) temporal and (b) spatial speckle contrast analysis. The symbols represent experimental data and the solid lines are the corresponding fits to Eq. (4).

From our experimental data, for predominantly dynamic speckle, the speckle contrast depends on the spatial sampling of the speckle pattern, for both temporal and spatial speckle-contrast analysis. Equation (4) fits the temporal- and spatial-contrast data well for all experimental values of N (Fig. 3), although the fit is less accurate for the latter.

For dynamic scattering, K increases with N (Fig. 4). A notable difference between the data in Fig. 4 and those from [8] is that K increases even for N values greater than two. In other words, even when the Nyquist criterion is met a reduction in speckle contrast remains due to the spatial averaging of the speckle pattern due to the finite pixel-size. With a static scattering substrate, the data from [8] reached a plateau value for all N > 2. As with experimental data collected from a substrate with static optical scatterers [8], our data demonstrate that speckle contrast from dynamic scatterers depends on N. Since most experimental studies involve use of LSI to assess relative changes in blood flow, an important practical question is to assess the effect of N on the relative flow-speed measurements (i.e., relative changes in SFI).

#191144 - $15.00 USD Received 24 May 2013; revised 25 Jul 2013; accepted 26 Jul 2013; published 30 Aug 2013

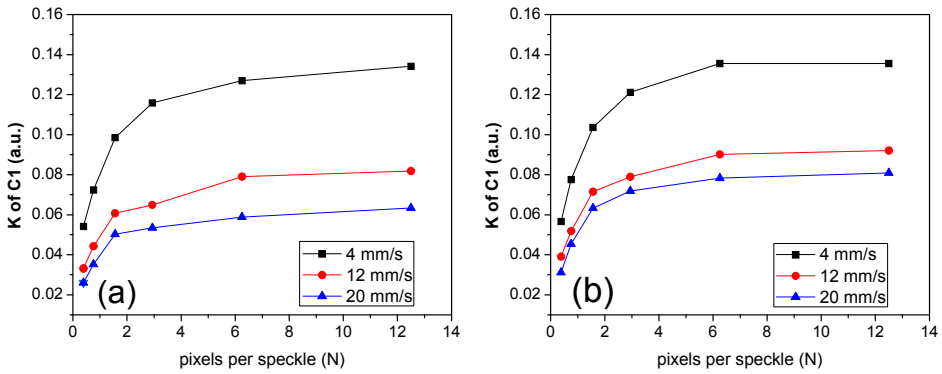

Fig. 4. Speckle contrast as a function of the pixels-per-speckle ratio for (a) temporal and (b) spatial analysis. Note that the value of K increase even when the Nyquist criterion of two pixels per speckle is satisfied.

Our experimental data demonstrate that, over a large range of N values (0.39 to 12.5) and flow speeds (up to 20 mm/s), the relative change in SFI is the same (Fig. 5). For example, the ratio in SFI values between channels C1 and C3 is equal to ~2 for each of the N values used in this study; this ratio is in agreement with the expected ratio in flow speed based on the relative dimensions of the two channels.

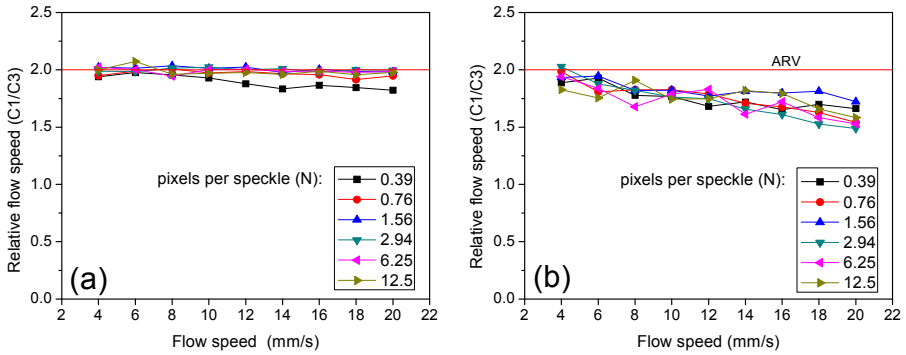

Fig. 5. Relative flow speed [i.e., (SFI in C1)/(SFI in C3)] is only weakly dependent on N and actual flow speed. The dependence is noticeably weaker with the (a) temporal speckle contrast approach than with the (b) spatial speckle contrast approach.

Note that the C1/C3 ratio is more accurate using temporal contrast analysis (Fig. 5(a)) than with spatial contrast analysis (Fig. 5(b)). While the relative flow speed remains at a value of ~2 with temporal analysis, the relative speed decreases linearly with actual flow speed when spatial analysis is used. A similar trend was found for C1/C5 ratio, for this time the relative flow speed remains at a value slightly below 4 (probably due to friction) for the temporal algorithm and it decays linearly for the spatial analysis. The same result was observed using various sliding-window sizes (5x5, 7x7 and 9x9) [18].

This difference in behavior of the spatial and temporal speckle-contrast algorithms is an unexpected finding. Recently Parthasarathy *et al.* [12, 19] suggested that the spatial algorithm is more sensitive to the static component of the scattered light than is the temporal algorithm. Based in this hypothesis, we explain the linear decay shown in Fig. 5(b) as follows. Based on Eq. (2) and assuming no noise, we define the spatial speckle contrast in channel C1 ($K_{S,C1}$) as:

$$K_{s,C1}^2 = \beta\rho^2 \frac{e^{-2x}-1+2x}{2x^2} + 4\beta\rho(1-\rho)\frac{e^{-x}-1+x}{x^2} + (1-\rho)^2 \qquad (5)$$

#191144 - $15.00 USD Received 24 May 2013; revised 25 Jul 2013; accepted 26 Jul 2013; published 30 Aug 2013

Similarly, the spatial speckle contrast in channel C3 is:

$$K_{s,C3}^2 = \beta\rho^2 \frac{e^{-2(x/2)} - 1 + 2(x/2)}{2(x/2)^2} + 4\beta\rho(1-\rho)\frac{e^{-(x/2)} - 1 + (x/2)}{(x/2)^2} + (1-\rho)^2 \qquad (6)$$

The last two terms in Eq. (5) account for the static component of the scattered light. Assuming that the temporal speckle-contrast algorithm is insensitive to the static component of the scattered light, we define the temporal contrast for C1 and C3 as:

$$K_{t,C1}^2 = \rho\beta \frac{e^{-2x} - 1 + 2x}{2x^2} \qquad (7)$$

$$K_{t,C3}^2 = \rho\beta \frac{e^{-2(x/2)} - 1 + 2(x/2)}{2(x/2)^2} \qquad (8)$$

In the long-exposure regime (e.g., $T >> \tau_c$) the relative flow speed (RFS) is:

$$RFS = \frac{SFI\_C1}{SFI\_C3} = \frac{K_{C1}^2}{K_{C3}^2} \qquad (9)$$

where SFI in C1 is defined as $SFI\_C1 = 1/(TK^2_{C1})$ and the SFI in C3 as $SFI\_C3 = 1/(TK^2_{C3})$. Note that Eq. (9) does depend on ρ for the spatial algorithm (Eqs. (5) and (6)), but it does not depend on ρ for the temporal algorithm (Eqs. (7) and (8)), moreover both algorithm predict the same RFS when ρ = 1. Figure 6 shows Eq. (9) plotted versus x (which is proportional to flow speed) for the temporal algorithm (solid lines which are overlaped) and the spatial algorithm (dashed lines) for three values of ρ.

For values of ρ = 0.98, 0.99, and 1.00, the RFS associated with temporal speckle-contrast analysis is independent of both ρ and x; the curves for ρ = 0.98 to 1.00 overlap. On the other hand, for the same values of ρ, the RFS associated with spatial speckle-contrast analysis are sensitive to the value of x. Note that these trends are similar to those observed experimentally (Fig. 5).

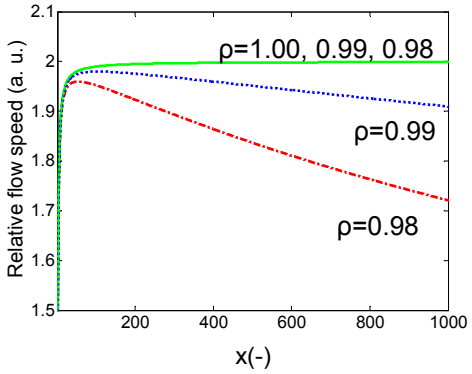

Fig. 6. RFS as a function of x (which is proportional to SFI) for three values of ρ. It is assumed that the actual RFS is two. The RFS associated with the temporal speckle-contrast algorithm is two for different values of x (continuous line), for ρ = 0.98 to 1.00. However, with spatial speckle-contrast analysis, the RFS decreases with x for all values of ρ below unity.

4. Conclusions

Our in-vitro experimental data collected from a dynamic-scattering phantom demonstrate that speckle contrast increases with the ratio of pixel size to speckle size, even at values beyond the Nyquist sampling criterion of N = 2. For monitoring of relative changes in blood flow,

#191144 - $15.00 USD Received 24 May 2013; revised 25 Jul 2013; accepted 26 Jul 2013; published 30 Aug 2013

however, the relative change in SFI is minimally affected by N and flow speed, over a large range of values for the two parameters. Use of the temporal speckle-contrast algorithm, is more accurate at assessing relative changes in blood flow, especially at faster flow speeds, than the commonly-used spatial algorithm. Based on these findings, we recommend that, for measurement of relative changes in blood flow in samples with minimal motion artifact, such as a rodent brain fixed in a stereotactic frame, that the temporal LSCI algorithm be used.

Acknowledgments

This research was supported in part by CONACYT (Mexico) under the grant CB-2010-156876-F, the Arnold and Mabel Beckman Foundation, and the National Institutes of Health (P41 EB015890, R01 DE022831, R01 HD065536).

#191144 - $15.00 USD Received 24 May 2013; revised 25 Jul 2013; accepted 26 Jul 2013; published 30 Aug 2013